

# Testing the repeatability of TILT technology in RTK GNSS (GPS/GLONASS/Galileo/Beidou) by using building corners

A. PIRTI

*Department of Geomatic Engineering, Yildiz Technical University, Istanbul, Turkey*

(Received: 9 March 2024; accepted: 5 November 2024; published online: 3 March 2025)

**ABSTRACT** The swift advancement of sensor fusion methodologies in global navigation satellite systems (GNSSs) and inertial measurement units (IMUs) presents a significant prospect to enhance the practicality, efficiency, and user experience of very precise real time kinematic (RTK) GNSS positions. Now that Topcon Integrated Levelling Technology (TILT) compensation technology is available, GNSS RTK can be used more effectively and adaptably in scenarios with greater constraints by automatically adjusting pole tilt from plumb. However, most conventional tilt compensation methods need laborious on-site calibrations and are vulnerable to magnetic disturbances. In addition, it is common for the tilt correction range to be 15 degrees. This research, instead, looks at the precision and repeatability that the RTK GNSS was able to achieve on 20 December 2023, using various satellite configurations. The United States' National Standard for Spatial Data Accuracy (NSSDA) governs how spatial data accuracy is reported. At 15-degree tilt angles, where a three dimensional positioning precision of approximately 1-15 cm that is possible in our investigation, the receiver IMU-based tilt correction is appropriate.

**Key words:** TILT, GNSS, accuracy, repeatability, corners of the building.

## 1. Introduction

Many problems are involved in the measuring of building corners with global navigation satellite system (GNSS) receivers. Except for reasons such as multipath or signal blockage, it is impossible to determine the correct coordinates due to the offset between the GNSS receiver wall contact point and the antenna phase centre. The biggest con of an inertial measurement unit (IMU) tilt sensor is the compensation that may occur when measuring points with an angle. When accuracy is required to be the highest possible, the best solution is to not keep a real time kinematic (RTK) GNSS receiver with an IMU tilt sensor at an angle of 60°. If a deviation of a few centimetres is irrelevant, then, the matter is of no concern. IMUs typically consist of an accelerometer, gyroscope, and, sometimes, GNSS or magnetometer equipment (Nichols and Talbot, 1996; Jekekli, 2001; Hong *et al.*, 2005; Kurtovic and Pagan, 2009; Groves, 2013; Luo *et al.*, 2017). To compute movement and monitor a device's location and orientation in space, an IMU detects the inertial gravitational forces inside the object. While an inertial navigation system (INS) does not depend on external signals like GNSS, it performs the same functions as an IMU. Only in relation to a specified starting point can the absolute attitude be computed using the internal sensors. Many papers have been published on the determination of the coordinates of building corners (Jekeli, 2001; Hong *et al.*, 2005; Pedley, 2012; Groves, 2013; Krzyżek, 2014, 2015a, 2015b, 2015c, 2017; Luo *et al.*, 2018; Sveinung *et al.*,

2021; Pirti and Yucel, 2023; Gučević *et al.*, 2024). However, in this study, the Topcon Integrated Levelling Technology (TILT) system utilised by surveying RTK GNSSs (GPS/GLONASS/Galileo/BeiDou) was repeatedly examined with 15° angle values on 13 different times of the day (20 December 2023). The aim of this study was to determine if the actual method TILT used in practice for the execution of building edge/corner surveys was effective or not (by using the NSSDA). This study investigates the accuracy and repeatability of RTK GNSSs (TILT) by comparing the coordinates of a group of test points (B1, B2, B3, B4, and B5 points) determined from an RTK GNSS and by using a total station.

## 2. Materials and methods

Stake-out or measurement of points, when the survey rod is tilted or tipped, is possible with a GNSS receiver equipped with an IMU tilt adjustment. This facilitates precise measuring without requiring the antenna to be levelled, resulting in quicker and more effective field operations.

To continually detect its location, rotation, and degree of tilt, as well as to compensate for any tilt, the receiver IMU employs data from a GNSS, acceleration sensors (accelerometers), and rotational sensors (gyroscopes). When the pole is IMU tilt compensated, it may be tilted at any angle, and the software can compute the tilt angle and tilt distance to find the pole tip location on the ground. IMU tilt correction may be utilised for any measurement technique (apart from observed control point) and is “always on” when enabled. When measuring an observed control point, the receiver automatically switches to GNSS-only mode and the GNSS eBubble appears automatically, if it is enabled (Yang and Freestone, 2016, 2017; Yang and Gilbertson, 2016; Pirti and Yucel, 2023).

A whole new working method is made possible with IMU tilt correction, which enables an accurate and rapid measuring of points when walking or standing, without the need to level the pole. Focus on the necessary location for the pole tip is particularly helpful during stake-out. Difficult spots, such as pipe inverts and building corners, can also be properly surveyed with this method. When the pole tip is steady, the receiver automatically adjusts for “pole wobble”, so that pole movement while measuring is of no concern.

IMU tilt correction may be employed in locations where magnetic disturbance may be present, such as those surrounding heavy equipment, steel-reinforced structures, or automobiles. This as its performance remains unaffected by magnetic interference. IMU sensors always determine the receiver orientation and tilt angle. When used in conjunction with GNSS, the receiver can continually calculate its location and adjust for tilt to any degree.

No specific measuring technique is needed for IMU tilt adjustment. IMU tilt compensation is always enabled when roving, navigating, or measuring points with any measurement technique. The degree of tilt of the receiver is electronically represented by the GNSS eBubble. When measuring a point, use the GNSS eBubble to make sure the pole is vertical, steady, and stable. In recent decades, electronic bubbles, or “eBubbles” emerged, using microelectromechanical (MEMS) tilt sensors along with various methods to apply an orientation to compute the position of the pole tip relative to the phase centre of the GNSS antenna. In survey mode, GNSS receivers and tilt features are enabled. Using a receiver with IMU tilt compensation enables points to be measured or staked out while the survey rod is tilted or tipped. This enables accurate measurements to be taken without having to level the antenna and a focus on the pole tip during stakeout, allowing for faster, more efficient work in the field. Enable eBubble functions in the survey style so that you can use the GNSS eBubble to help you keep the receiver's integrated

antenna level when measuring a point if you are working in GNSS-only mode. The GNSS eBubble is not shown when the IMU is aligned. Robust and high-sensitivity tracking of GNSS signals in all frequency bands is crucial for high-precision RTK positioning with tilt compensation, especially at large tilt degrees. The elevation angle of the incoming GNSS signal, with regard to the antenna horizon, drops by  $t$ , from  $\alpha$  (vertical pole) to  $\beta$  (tilted pole), if the pole is tilted away from a satellite by  $t$  degrees, as shown in Fig. 1. The greater tilt  $t$ , the lower angle  $\beta$  for a given elevation angle of  $\alpha$ . This suggests that, depending on the tilt angle, a GNSS signal received at a high elevation angle during traditional RTK surveying with a vertical pole may change into a low elevation angle during the tilt compensation scenario. Moreover, multipath or surrounding interferences cause an increase in the receipt of noise signals when performing tilt-compensated RTK measurements at building corners or in close proximity to walls and fences. The GNSS receivers have sophisticated signal tracking capabilities to meet these problems and offer the highest number of observations possible for tilt-compensated RTK solutions (Tittertan and Weston, 2004; Wolf and Ghialini, 2008; Topcon, 2022; Pirti and Yucel, 2023).

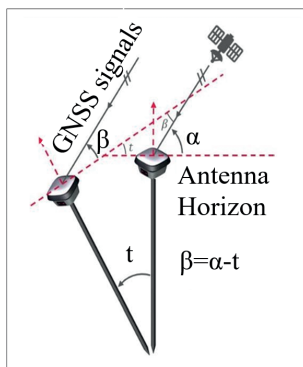


Fig. 1 - When tilting a pole away from the satellite, the incoming GNSS signal elevation angle decreases ( $t$  = tilt angle,  $\alpha$  = satellite elevation angle for vertical pole,  $\beta$  = satellite elevation angle for tilted pole).

An IMU tilt sensor in an RTK GNSS receiver can be really helpful as it significantly reduces the surveying time.

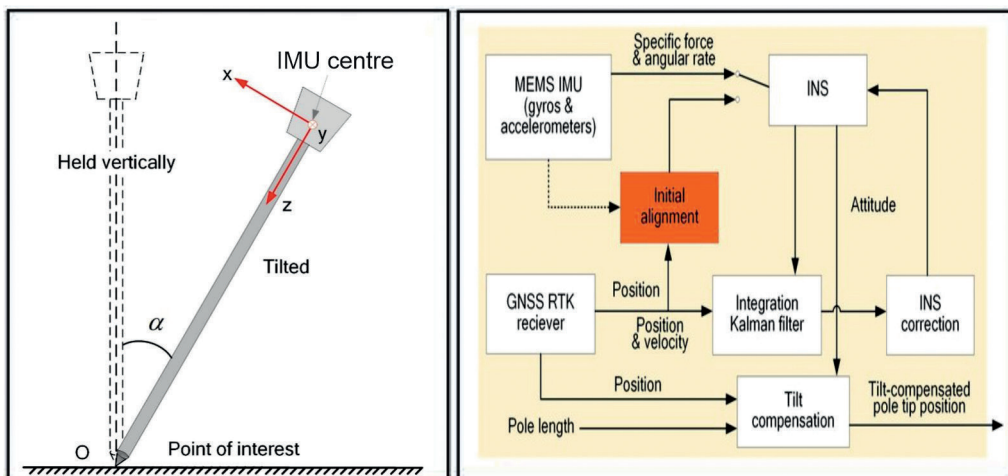


Fig. 2 - Illustration of TILT system and working schema.

Fig. 3 shows both an RTK GNSS receiver with a tilt compensation function and the configuration of the IMU body frame (b-frame, lateral view). For analysis purposes, the IMU measurement centre is assumed to coincide with the GNSS antenna phase centre (APC) (see Figs. 2 and 3).

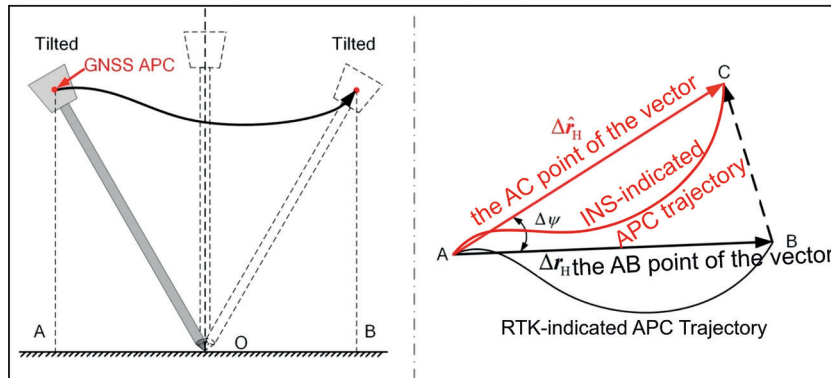


Fig. 3 - INS and RTK GNSS receivers.

Fig. 3 shows the illustration of the proposed INS alignment principle for tilted RTK GNSS receivers. The alignment involves shifting the pole from tilt position A to tilt position B. The INS- and RTK-indicated trajectories are similar in shape in the horizontal plane (top view) due to the existence of  $t$  (Tersus GNSS, 2021; Topcon, 2022).

### 3. Description of experiments

To investigate these problems, experiments were carried out in the Davutpaşa region (Yıldız Technical University Campus), near Istanbul, in Turkey. For this purpose, two reference points (T1 and T2) were located in the study area (clear-line of sight) (Figs. 4 and 5). Static GNSS surveys determined the coordinates of T1 and T2. On 18 December 2023, for at least 1.5 hours, the static data of the T1 and T2 stations were recorded. The cut-off elevation mask angle for the static survey was set to  $10^\circ$ , and the data-receiving and processing rates were set to 30 s. In the testing method, between 19 and 25 GNSS satellites were seen, and their locations were generally normal. For the static survey, the position dilution of precision (PDOP) ranged from 0.92 to 1.27. For data processing and network changes, Topcon Magnet Tools v.8.0.0 software was used. Table 1 shows that, during the adjustment phase, the PALA station (ISKI-CORS) ITRF 20 coordinates were fixed. Table 1 displays the coordinates and standard deviations (SDs) of these two reference locations (T1 and T2).

Furthermore, the five corners of the one-two-storey structures, about 7-9 m high, in the study area were denoted by points B1, B2, B3, B4, and B5 (Fig. 4). The horizontal accuracies obtained with the three different positioning methods are as follows: 3 mm + 0.4 ppm (static mode, Topcon Hiper VR receivers), 5 mm + 0.5 ppm (RTK), and 1.3 mm/ $^\circ$  tilt if tilt  $\leq 10^\circ$  and 1.8 mm/ $^\circ$  tilt if tilt  $> 10^\circ$  (compensator tilt sensor<sup>1</sup>). The vertical accuracies of the first two methods are 5 mm + 0.5 ppm (static mode, Topcon Hiper VR receivers) and 10 mm + 0.8 ppm (RTK), respectively.

<sup>1</sup> The maximum angle at which tilt correction is recommended is  $15^\circ$ .



Fig. 4 - The five corners of two buildings in the study region.



Fig. 5 - The B1, B2, B3, B4, and B5 corner points (panels a and b) and T1 and T2 reference points (panels c and d) in the study region and TILT surveying (panel e).

Table 1 - SD and coordinate values of the three points obtained by using static surveys.

Point	Grid northing (m)	Grid easting (m)	Elevation (m)	SD N (m)	SD E (m)	SD h (m)
<b>PALA</b>	4550678.003	412881.99	170.561	0	0	0
<b>T1</b>	4543654.060	406382.345	111.119	0.002	0.002	0.004
<b>T2</b>	4543760.218	406335.513	109.705	0.002	0.002	0.004

For each site, 13 RTK GNSS surveys were conducted at different times of the day, with considerable alterations made to the satellite configuration to ensure the independence of the findings (Tables 2, 3, 4, 5, and 6).

#### 4. Results

Based on GPS+GLONASS+Galileo+Beidou satellite configurations and the T2 reference point, RTK GNSS surveys were carried out on 20 December 2023, between 9:26:53 and 9:44:28 hours, with 15° tilt angles. We were able to retrieve the coordinates for building corner point B1. The recording interval of one second and the epoch value of 10 were selected. During this period, 4-5 GPS, 3-5 GLONASS, 4-5 Galileo, and 1-3 Beidou satellites were discovered. The range of PDOP values for this time frame was 1.206 to 1.819.

Table 2 - RTK GNSS surveys for point B1 conducted using a Topcon Hiper VR receiver.

20 December 2023								
Point	Satellites	Tilt angle	Y	X	h	Epoch	Sat. number	PDOP
<b>B1</b>	GNSS	15°	406369.691	4543617.227	110.916	10	9	1.819
<b>B1</b>	GNSS	15°	406369.683	4543617.259	110.893	10	10	1.44
<b>B1</b>	GNSS	15°	406369.689	4543617.185	110.890	10	12	1.219
<b>B1</b>	GNSS	15°	406369.678	4543617.223	110.887	10	11	1.31
<b>B1</b>	GNSS	15°	406369.683	4543617.248	110.887	10	11	1.349
<b>B1</b>	GNSS	15°	406369.711	4543617.191	110.889	10	11	1.246
<b>B1</b>	GNSS	15°	406369.684	4543617.245	110.885	10	10	1.318
<b>B1</b>	GNSS	15°	406369.685	4543617.185	110.892	10	13	1.206
<b>B1</b>	GNSS	15°	406369.687	4543617.180	110.885	10	13	1.298
<b>B1</b>	GNSS	15°	406369.666	4543617.229	110.873	10	13	1.277
<b>B1</b>	GNSS	15°	406369.666	4543617.244	110.870	10	12	1.321
<b>B1</b>	GNSS	15°	406369.651	4543617.249	110.874	10	11	1.457
<b>B1</b>	GNSS	15°	406369.651	4543617.223	110.889	10	11	1.619

**Epoch:** The measurement interval of a GPS/GNSS receiver for coordinate estimation.

Table 3 shows the results of RTK surveys conducted on 20 December 2023, between 9:49:53 and 10:06:04 hours, using 15° tilt angles. The coordinates of the B2 building corner point were obtained using satellite configurations (GPS+GLONASS+Galileo+Beidou) and the T2 reference point. One second was chosen as the recording interval, and 10 was the epoch value. During this

time, 4-5 GPS, 2-3 GLONASS, 2-3 Galileo, and 1-3 Beidou satellites were detected. PDOP values during this time period ranged from 1.169 to 1.883.

Table 3 - RTK GNSS surveys for point B2 conducted using a Topcon Hiper VR receiver.

20 December 2023								
Point	Satellites	Tilt angle	Y	X	h	Epoch	Sat. number	PDOP
B2	GNSS	15°	406412.136	4543582.617	110.979	10	10	1.472
B2	GNSS	15°	406412.171	4543582.594	110.944	10	12	1.410
B2	GNSS	15°	406412.156	4543582.619	110.984	10	11	1.341
B2	GNSS	15°	406412.151	4543582.625	110.971	10	14	1.169
B2	GNSS	15°	406412.186	4543582.561	110.970	10	11	1.502
B2	GNSS	15°	406412.209	4543582.584	110.972	10	9	1.883
B2	GNSS	15°	406412.211	4543582.600	110.965	10	9	1.659
B2	GNSS	15°	406412.185	4543582.560	110.993	10	12	1.383
B2	GNSS	15°	406412.211	4543582.603	110.966	10	12	1.461
B2	GNSS	15°	406412.215	4543582.601	110.975	10	11	1.623
B2	GNSS	15°	406412.209	4543582.583	110.973	10	11	1.365
B2	GNSS	15°	406412.215	4543582.574	110.962	10	11	1.424
B2	GNSS	15°	406412.202	4543582.584	110.985	10	11	1.623

On 20 December 2023, between 10:07:31 and 10:22:08 hours, RTK surveys were carried out using satellite configurations (GPS+GLONASS+Galileo+Beidou) and the T2 reference point, with a chosen 15° tilt angle. We were able to collect the corner point coordinates for the B3 building. The epoch value was 10, and the recording interval was set at one second. Satellite detections during this period included 4-5 GPS, 2-3 GLONASS, 2-3 Galileo, and 1-3 Beidou satellites. During this period, the PDOP values ranged from 1.134 to 1.514.

Using satellite configurations (GPS+GLONASS+Galileo+Beidou) and the T2 reference point, RTK surveys were conducted on 20 December 2023, between 10:23:10 and 10:37:33 hours, selecting a 15° tilt angle. The coordinates of the B4 building corner point were obtained. One second was chosen as the recording interval, and 10 was the epoch value. During this time, 4-5 GPS, 2-3 GLONASS, 2-3 Galileo, and 1-2 Beidou satellites were detected. PDOP values during this time period ranged from 1.311 to 1.915.

RTK surveys were conducted on 20 December 2023, between 10:38:37 and 10:53:14 hours, using satellite configurations (GPS+GLONASS+Galileo+Beidou) and the T2 reference point, with a 15° tilt angle. The coordinates of the B5 building corner point were determined. The recording interval of one second and the epoch value of 10 were selected. 4-5 GPS, 2-3 GLONASS, 2-3 Galileo, and 1-2 Beidou satellites were found during this period. Throughout this timeframe, the PDOP values ranged from 1.342 to 2.663.

The use of GNSS facilitated the quick development of positioning technology. The employment of many constellations is important because of the rise of visible satellites, which may improve satellite geometry and increase the number of observables that are accessible (Tables 2, 3, 4, 5, and 6). When the data from all constellations were merged, all configurations showed better location accuracy when taking into account the use of GPS/GLONASS/Gaileo/Beidou data (Wolf and Ghiliani, 2008). The GNSS technology offers strong RTK position availability and dependability by using all available GPS, GLONASS, Galileo, and BeiDou signals.

Table 4 - RTK GNSS surveys for point B3 conducted using a Topcon Hiper VR receiver.

20 December 2023								
Point	Satellites	Tilt angle	Y	X	h	Epoch	Sat. number	PDOP
B3	GNSS	15°	406378.725	4543573.177	110.609	10	11	1.241
B3	GNSS	15°	406378.743	4543573.150	110.601	10	11	1.158
B3	GNSS	15°	406378.790	4543573.174	110.590	10	11	1.145
B3	GNSS	15°	406378.784	4543573.191	110.592	10	10	1.225
B3	GNSS	15°	406378.792	4543573.174	110.602	10	11	1.274
B3	GNSS	15°	406378.776	4543573.166	110.577	10	11	1.134
B3	GNSS	15°	406378.777	4543573.167	110.560	10	11	1.200
B3	GNSS	15°	406378.793	4543573.210	110.581	10	12	1.204
B3	GNSS	15°	406378.739	4543573.151	110.570	10	12	1.247
B3	GNSS	15°	406378.765	4543573.182	110.575	10	11	1.288
B3	GNSS	15°	406378.773	4543573.174	110.594	10	11	1.424
B3	GNSS	15°	406378.791	4543573.181	110.582	10	11	1.372
B3	GNSS	15°	406378.775	4543573.192	110.548	10	10	1.514

Table 5 - RTK GNSS surveys for point B4 conducted using a Topcon Hiper VR receiver.

20 December 2023								
Point	Satellites	Tilt angle	Y	X	h	Epoch	Sat. number	PDOP
B4	GNSS	15°	406367.390	4543562.409	107.656	10	9	1.915
B4	GNSS	15°	406367.400	4543562.454	107.638	10	11	1.490
B4	GNSS	15°	406367.380	4543562.481	107.635	10	11	1.430
B4	GNSS	15°	406367.385	4543562.408	107.648	10	11	1.536
B4	GNSS	15°	406367.373	4543562.518	107.653	10	11	1.453
B4	GNSS	15°	406367.378	4543562.414	107.650	10	11	1.311
B4	GNSS	15°	406367.386	4543562.427	107.662	10	11	1.405
B4	GNSS	15°	406367.359	4543562.463	107.669	10	12	1.417
B4	GNSS	15°	406367.366	4543562.418	107.672	10	12	1.381
B4	GNSS	15°	406367.371	4543562.497	107.661	10	11	1.493
B4	GNSS	15°	406367.403	4543562.523	107.643	10	12	1.538
B4	GNSS	15°	406367.376	4543562.542	107.641	10	10	1.564
B4	GNSS	15°	406367.353	4543562.432	107.642	10	12	1.446

## 5. Analysis of RTK GNSS (TILT) accuracy-repeatability

In this investigation, RTK GPS/GPS-GLONASS/GNSS measurements were made at building corner points B1, B2, B3, B4, and B5 at various times of the day (20 December 2023) using a 15° tilt angle. The precision and repeatability of the acquired coordinates were compared and examined. The experiment comprised five ground-marked locations (B1, B2, B3, B4, and B5), as previously mentioned. It should be noted that several satellite constellations and times of day were used for the studies. A cut-off elevation mask angle of 10° was used for the RTK GNSS surveys. The data acquisition (the act of receiving data) and processing rate (the amount of raw

Table 6 - RTK GNSS surveys for point B5 conducted using a Topcon Hiper VR receiver.

20 December 2023								
Point	Satellites	Tilt angle	Y	X	h	Epoch	Sat. number	PDOP
B5	GNSS	15°	406411.860	4543537.739	110.872	10	9	1.685
B5	GNSS	15°	406411.890	4543537.735	110.884	10	11	1.839
B5	GNSS	15°	406411.889	4543537.722	110.868	10	9	1.377
B5	GNSS	15°	406411.902	4543537.751	110.871	10	8	1.743
B5	GNSS	15°	406411.904	4543537.761	110.864	10	10	1.342
B5	GNSS	15°	406411.887	4543537.762	110.851	10	9	1.405
B5	GNSS	15°	406411.843	4543537.717	110.842	10	8	1.869
B5	GNSS	15°	406411.894	4543537.732	110.874	10	9	2.122
B5	GNSS	15°	406411.897	4543537.791	110.906	10	9	1.840
B5	GNSS	15°	406411.924	4543537.834	110.988	10	9	2.457
B5	GNSS	15°	406411.918	4543537.758	110.829	10	10	2.491
B5	GNSS	15°	406411.888	4543537.770	110.807	10	8	2.700
B5	GNSS	15°	406411.862	4543537.754	110.798	10	8	2.663

materials or process intermediates used or products made by any equipment, source operation, or control apparatus) were set to one second and 10 epochs, respectively. Utilising Topcon Hiper VR receivers, the integer ambiguity was solved for each point, within the range of 1 to 10 s. The first survey was conducted on 20 December 2023 and the other surveys were conducted on the same day (morning, noon, and afternoon) using identical RTK GNSS receivers. The coordinate discrepancies between the five places in the RTK GNSS survey findings are shown in Figs. 6 and 7. Additionally, included in the figures are the mean and SD of the coordinate differences

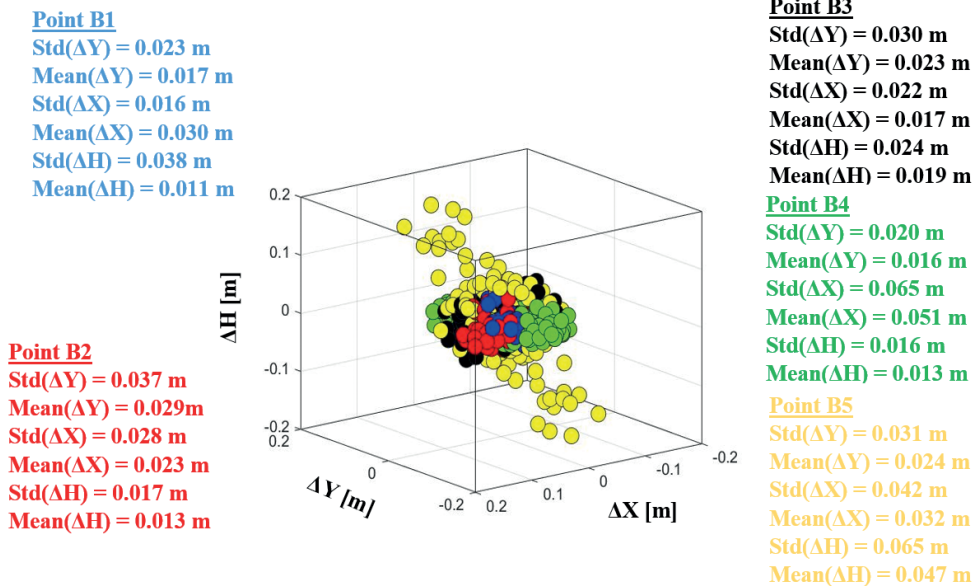


Fig. 6 - Comparison of the B1, B2, B3, B4, B5 corner point coordinates obtained from RTK GNSS surveys on 20 December 2023 by using the T2 reference point.

between the first and the subsequent surveys. The horizontal coordinates of the locations, as independently established by these tests, seem to be similar when the outcomes of the RTK GNSS surveys are compared, with occasional SDs ranging from a few millimetres to 20 cm. The height component, on the other hand, varied less consistently throughout all RTK GNSS sessions, sometimes by up to 20 cm at the same locations.

Additionally, Fig. 6 displays the coordinate discrepancies between the B1, B2, B3, B4, and B5 points (marked in the corners of the two buildings) of the RTK GNSS survey data on 20 December 2023. For the five points, the findings from the remaining five RTK GNSS surveys are compared with the coordinates acquired from the first RTK GNSS scan for B1, B2, B3, B4, and B5. Overall, the five location coordinates (northing and easting) were satisfactory, with mean values of less than 5.1 cm and SD values of less than 6.5 cm. Height variations between RTK GNSS readings of up to 6.5 cm occurred at the same location. Fig. 6 shows the mean and SD of the heights of the five locations, which were 2.2-2.6 cm and 1.6-6.5 cm, respectively.

## 6. Total station surveys and comparisons

By comparing RTK GNSS data with coordinates obtained from terrestrial measurements, data correctness may be ascertained. A complete station was used to measure the angles and distances between the sites in order to compare the outcomes of the RTK GNSS techniques. For the total station surveys, the T1 and T2 reference sites were used as control points (Fig. 3). By setting reference point PALA (ISKI-CORS), the T1 and T2 coordinates were calculated using the static GNSS data (measurement durations of about 90 minutes). Five corner points (B1, B2, B3, B4, and B5) were seen from the T1 and T2 locations, as was previously mentioned. The coordinates of the five locations were ascertained by observing the horizontal angles, zenith angles, horizontal distances, and slope distances using Topcon GTS-701 (angle accuracy: 2", distance measurement accuracy: 2 mm + 2 ppm). The coordinate values for the five stations (B1, B2, B3, B4, and B5), derived from total station surveys (using T1 and T2 reference points), are shown in Table 7.

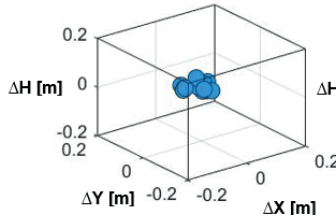
Table 7 - Coordinate values of points B1, B2, B3, B4 and B5 obtained by using a total station.

Total station			
Point	Northing (m)	Easting (m)	Elevation (m)
B1	406369.647	4543617.211	110.883
B2	406412.129	4543582.562	110.978
B3	406378.701	4543573.152	110.582
B4	406367.305	4543562.539	107.650
B5	406411.775	4543537.745	110.838

For points B1, B2, B3, B4, and B5, the RTK GNSS results were 1 to 5 cm lower in height and 1 to 20 cm lower in horizontal coordinates than the total station results (Fig. 7). With an SD of less than 11 cm and a mean of less than 7 cm, the coordinates (northing and easting) of the B1 point were generally satisfactory. Less consistently, height variations between RTK GNSS readings of up to 5 cm occurred at the same location. Fig. 8 shows that the height of the B1 point had an

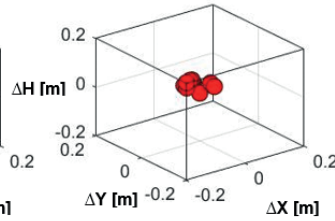
**Point B1**

Std( $\Delta Y$ ) = 0.017 m  
 Mean( $\Delta Y$ ) = 0.032 m  
 Std( $\Delta X$ ) = 0.028 m  
 Mean( $\Delta X$ ) = 0.027 m  
 Std( $\Delta H$ ) = 0.011 m  
 Mean( $\Delta H$ ) = 0.009 m



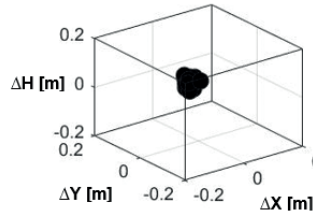
**Point B2**

Std( $\Delta Y$ ) = 0.027 m  
 Mean( $\Delta Y$ ) = 0.060 m  
 Std( $\Delta X$ ) = 0.021 m  
 Mean( $\Delta X$ ) = 0.031 m  
 Std( $\Delta H$ ) = 0.012 m  
 Mean( $\Delta H$ ) = 0.010 m



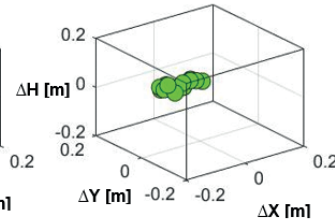
**Point B3**

Std( $\Delta Y$ ) = 0.022 m  
 Mean( $\Delta Y$ ) = 0.065 m  
 Std( $\Delta X$ ) = 0.016 m  
 Mean( $\Delta X$ ) = 0.028 m  
 Std( $\Delta H$ ) = 0.017 m  
 Mean( $\Delta H$ ) = 0.004 m



**Point B4**

Std( $\Delta Y$ ) = 0.015 m  
 Mean( $\Delta Y$ ) = 0.049 m  
 Std( $\Delta X$ ) = 0.047 m  
 Mean( $\Delta X$ ) = 0.023 m  
 Std( $\Delta H$ ) = 0.012 m  
 Mean( $\Delta H$ ) = 0.014 m



**Point B5**

Std( $\Delta Y$ ) = 0.023 m  
 Mean( $\Delta Y$ ) = 0.114 m  
 Std( $\Delta X$ ) = 0.031 m  
 Mean( $\Delta X$ ) = 0.023 m  
 Std( $\Delta H$ ) = 0.048 m  
 Mean( $\Delta H$ ) = 0.040 m

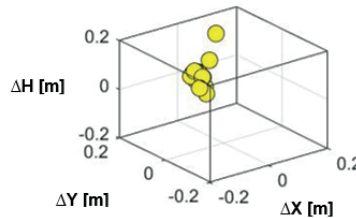


Fig. 7 - Comparison of the B1, B2, B3, B4, and B5 coordinates obtained from RTK GNSS surveys on 26 May 2022 and 1 June 2022 with the coordinates of points B1, B2, B3, B4, and B5 obtained from the T1 and T2 reference points by using a total station.

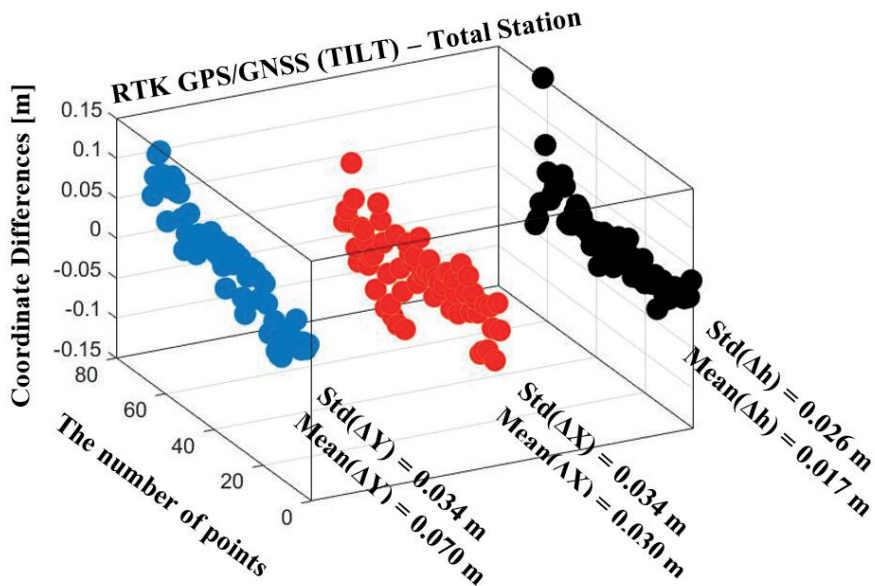


Fig. 8 - Comparison of the coordinates of the five building corners (B1, B2, B3, B4, and B5) on 20 December 2023 using T1 and T2 reference points (Topcon Hiper-VR) with the coordinates of the five building corners (B1, B2, B3, B4, and B5) using a total station.

SD of 1.8-3.5 cm and a mean value of 2.2-2.6 cm. Upon comparing the RTK GNSS findings with the total station surveys, the differences were found to be greater in height (1-35 cm) and less in horizontal coordinates (1-20 cm) for the B2 location (Fig. 7). With an SD of less than 7 cm and a mean of less than 13 cm, the coordinates (northing and easting) of the B1 point were generally satisfactory. With SDs of up to 20-35 cm at the same location between RTK GNSS readings, the height component showed less consistency. The height of the B1 point had an SD of 1.9-6.3 cm and a mean of 18-21 cm, as shown in Fig. 7.

All of the findings also demonstrate that buildings hindered the RTK GNSS location as they regularly interfered with radio signals and prevented low-medium satellite transmissions. Therefore, signal blocking caused by buildings may be regarded as the primary issue influencing the usage of RTK GNSS in regions with buildings, even in the presence of adequate satellite windows. Fig. 8 displays the average SDs of the five tests of building corner points B1, B2, B3, B4, and B5 in the northing, easting, and elevation coordinate directions. With a SD of less than 3.5 cm, the coordinates (northing and easting) of all five corner points were generally excellent. With a SD of 3 cm on average, a precise height accuracy was obtained in this study. However, the height component showed less consistency between the RTK sessions using the T2 reference point, with SDs as high as about 15 cm (Fig. 8). The results unequivocally demonstrate that the RTK GNSS method is a stable system and that the centimetre accuracy level is typically achievable under a variety of operational settings, given the dynamics of these tests and the changing geometry of satellites at the five corners of a building environment on a given day (Fig. 8).

## 7. Accuracy reporting for RTK GNSS experiments

The NSSDA is applied to completely georeferenced maps and digital geospatial data in raster, point, or vector format acquired from sources such as aerial photography, satellite imaging, and ground surveys. It is used by United States transportation organisations such as the Minnesota Department of Transportation. In order to estimate the positional accuracy of points on maps and in digital geospatial data with relation to georeferenced ground locations of greater precision, the NSSDA applies a statistical and testing approach. The root-mean-square error (RMSE) is used by the NSSDA to compute positional accuracy. The horizontal accuracy statistic worksheet is utilised if the planimetric accuracy, i.e. the X and Y accuracy, of the data set is being assessed (see Table 8). The vertical accuracy worksheet is used while evaluating height (H) accuracy (see Table 9). To compute the NSSDA statistic, the relevant tables (Tables 8 and 9) should be completed with the needed data (Positional Accuracy Handbook, 1999). To obtain the NSSDA statistic, the RMSE must be multiplied by the standard mean error at the 95% confidence level, which is 1.7308 for horizontal accuracy and 1.9600 for vertical accuracy. As can be seen in Tables 8 and 9, the difference between input  $X_{data}$  and check  $X_{check}$  equals  $\Delta X$ , and the square of  $\Delta X$  yields the "(1)"

Table 8 - Horizontal accuracy statistic worksheet.

	<b>(1) + (2)</b>
<b>SUM</b>	= (1) + (2)
<b>Average</b>	= SUM / n
<b>RMSE<sub>r</sub></b>	= $\sqrt{\text{Average}}$
<b>Accuracy per NSSDA</b>	= 1.7308 × RMSE <sub>r</sub>

Table 9 - Vertical accuracy statistic worksheet.

<b><math>\Delta H</math></b>	<b><math>\Delta H \times \Delta H</math></b>
<b>SUM</b>	<b>= (1)</b>
<b>Average</b>	<b>= SUM / n</b>
<b>RMSE<sub>r</sub></b>	<b>= <math>\sqrt{\text{Average}}</math></b>
<b>Accuracy per NSSDA</b>	<b>= 1.9600 <math>\times</math> RMSE<sub>r</sub></b>

output. Conversely, the difference between input  $Y_{\text{data}}$  and check  $Y_{\text{check}}$  equals  $\Delta Y$ , and the square of  $\Delta Y$  yields the "(2)" output, and the square root of the sum of the two inputs is obtained [(1) + (2)], (Positional Accuracy Handbook, 1999).

The repeated measurement of the same amount will often result in different results due to errors. The difference between two or more measurements of the same quantity is called a discrepancy. When there are minor differences between recurrent measurements, the general consensus is that there are relatively minor errors. Tables 10 and 11 (Positional Accuracy Handbook, 1999) provide report accuracy at the 95% confidence level for data generated by using methods that have been shown to yield data with certain horizontal and vertical accuracy values. According to the NSSDA, the results of the experiments provide horizontal and vertical accuracy results. Nonetheless, in the experiments the horizontal and vertical accuracy values per the NSSDA tend to be 2 cm and 20 cm (Tables 10 and 11).

Tables 10 and 11 indicate that five points have a greater horizontal positional accuracy. The vertical accuracy was determined by using the formula shown in Tables 8 and 9. The NSSDA may only use the vertical accuracy values of the experiment (see Tables 9 and 11). Upon examining all test points from the experiments, it is evident that the vertical positional errors are less than 15 cm. The accuracy of all test points in 13 tests was reported in this study in accordance with the NSSDA. Regarding the results, the horizontal and vertical accuracy of all test points are adequate (refer to Tables 10 and 11).

Table 10 - Horizontal accuracy statistic worksheet (between B1, B2, B3, B4, and B5 points).

Point		Exp.1 [cm]	Exp.2 [cm]	Exp.3 [cm]	Exp.4 [cm]	Exp.5 [cm]	Exp.6 [cm]	Exp.7 [cm]	Exp.8 [cm]	Exp.9 [cm]	Exp.10 [cm]	Exp.11 [cm]	Exp.12 [cm]
<b>B1</b>	<b>RMSE<sub>r</sub> accuracy per NSSDA</b>	3.3 5.6	5 8.6	4.3 7.4	3.2 5.5	4.5 7.7	4.7 8.2	4.4 7.5	4.8 8.2	4.5 7.9	3.8 6.6	4.6 8	4 6.8
<b>B2</b>	<b>RMSE<sub>r</sub> accuracy per NSSDA</b>	6.3 11	3.5 6	5 8.7	6.4 11	4.4 7.6	3.6 6.3	4 6.9	4.4 7.5	4 7	3.8 6.6	4.3 7.4	2.9 5.1
<b>B3</b>	<b>RMSE<sub>r</sub> accuracy per NSSDA</b>	5 8.7	4.8 8.2	3.1 5.3	3.1 5.4	2.9 5	2.7 4.6	4 7	4.6 8	3.6 6.2	25 4.4	3.2 5.5	2.9 5.2
<b>B4</b>	<b>RMSE<sub>r</sub> accuracy per NSSDA</b>	6.7 12	5.2 9	4.9 8.5	7.7 13	6.3 11	6 10	5.8 10	5 8.6	7 12	7.5 13	8.8 15	6.4 11
<b>B5</b>	<b>RMSE<sub>r</sub> accuracy per NSSDA</b>	4.7 8.2	4 7	4.8 8.3	3.8 6.7	3.7 6.4	4.8 8.2	5.9 10	5.6 10	8.1 14	5.5 9.6	4 6.9	4.4 7.5

Table 11 - Vertical accuracy statistic worksheet (between B1, B2, B3, B4 and B5 points).

Point		Exp.1 [cm]	Exp.2 [cm]	Exp.3 [cm]	Exp.4 [cm]	Exp.5 [cm]	Exp.6 [cm]	Exp.7 [cm]	Exp.8 [cm]	Exp.9 [cm]	Exp.10 [cm]	Exp.11 [cm]	Exp.12 [cm]
<b>B1</b>	<b>RMSE<sub>H</sub></b>	3	1.2	1.1	1	1	1.1	0.9	1.2	1.7	1.9	1.6	1.1
	<b>accuracy per NSSDA</b>	6	2.4	2.2	2	1.9	2.2	1.8	2.4	3.3	3.7	3.2	2.2
<b>B2</b>	<b>RMSE<sub>H</sub></b>	1.6	2.9	1.4	1	1.1	1.1	2	1.7	1.2	1.1	1.4	1.7
	<b>accuracy per NSSDA</b>	3	5.7	2.7	2	2.2	2.2	4	3.3	2.3	2.2	2.7	3.4
<b>B3</b>	<b>RMSE<sub>H</sub></b>	2.9	2.3	1.7	1.8	2.7	2.5	1.8	2	1.8	1.6	1.8	3.7
	<b>accuracy per NSSDA</b>	5.6	4.6	3.3	3.4	5.2	4.9	3.5	3.9	3.4	3.2	3.5	7.3
<b>B4</b>	<b>RMSE<sub>H</sub></b>	1.2	1.7	1.9	1.2	1	1.4	1.8	2.1	1.8	1.6	1.4	1.4
	<b>accuracy per NSSDA</b>	2.4	3.3	3.6	2.3	2	2.8	3.5	4.1	3.4	3.1	2.8	2.7
<b>B5</b>	<b>RMSE<sub>H</sub></b>	4.3	4.6	4.3	4.3	4.4	4.7	4.6	5.2	10.4	9.6	7	7.6
	<b>accuracy per NSSDA</b>	8.5	9	8.4	8.5	8.6	9.1	9	10.2	20.4	18.8	13.7	15

In recent years, there has been a growing recommendation for the use of GNSS technology as a means of monitoring displacements in structural health monitoring systems for structures and infrastructures. Recent studies have identified some critical issues in the use of satellite data for precision measurements in structures that are particularly sensitive to temperature-related effects (Ponzo *et al.*, 2024), including bridges. It is evident that these effects are more pronounced in structures with greater slenderness. Additionally, the magnitude of daily thermal fluctuations and the extent of solar radiation exposure on surfaces are crucial factors that must be taken in consideration.

Environmental factors can influence measurement accuracy by causing variations in the conditions under which measurements are taken.

Environmental factors such as temperature, humidity, pressure, light, and even magnetic fields can significantly influence the accuracy of measurements. For instance, in physics experiments, these factors can cause changes in the properties of the materials or equipment used, leading to variations in the results obtained. Ionospheric delay varies with solar activity, time of year, season, time of day, and location. This makes it very difficult to predict how much ionospheric delay will impact the calculated position. Variations in tropospheric delay are caused by changing humidity, temperature, and atmospheric pressure. On the other hand, weather phenomena, from dense cloud cover to solar storms, can significantly affect the performance of GNSS receivers. Weather conditions, including ionospheric disturbances, tropospheric delays, heavy rain, and snow can significantly affect GNSS receiver accuracy by distorting or delaying satellite signals. The solar cycle, also known as the solar magnetic activity cycle, sunspot cycle, or Schwabe cycle, is an almost periodic 11-year change in the Sun's activity measured in terms of variations in the number of observed sunspots on the Sun's surface. Over the period of a solar cycle, levels of solar radiation and ejection of solar material, the number and size of sunspots, solar flares, and coronal loops all exhibit a synchronised fluctuation from a period of minimum activity to a period of maximum activity, and back to a period of minimum activity (Ponzo *et al.*, 2024).

## 8. Conclusions

It is simply not possible to use the TILT approach in all situations or with the same degree of accuracy. As previously stated, surveyors are deeply concerned about quality assurance. The results of the experiments demonstrate that the TILT system accuracy, precision, and performance are significantly impacted by building, which, due to their reflection and blockage, negatively affect GNSS signals. In this study, all point coordinates were measured by means of a TILT receiver with excellent precision and accuracy in both the horizontal and vertical directions. The TILT system has a horizontal precision of 7-10 cm and a vertical accuracy of 7-15 cm, according to the investigation findings. These findings demonstrate that TILT technology is practical, efficient, and successful for placement and other uses in building corners and do not lead to unfavourable circumstances. Furthermore, with the Topcon Hiper VR receiver, fewer ground control points are needed for survey applications. The many comparisons between all the methodologies shown in this research demonstrate how well the accuracy of the TILT method and the total station survey match up. A 3D positioning precision of around 15 cm is possible in this investigation at tilt angles of 15°, where the receiver IMU-based tilt correction is relevant. The appropriate tilt for the GNSS receiver should be considered when using tilt-compensated equipment. Although, in general, a lower tilt angle is preferred, in rare circumstances, elevating the tilt may be beneficial or even necessary, depending on local restrictions.

**Acknowledgments.** We thank the staff of Topcon Paksoy Teknik Hizmetler in Turkey for the help and comments provided that greatly improved the manuscript. We thank Hafsa Altındağ, Sami Tapan, Ahmet Emre Garip, Mahmut BurakTansu (Graduation Thesis team-2023 Winter Semester). The multi-GNSS observation data from the CORS-TR, ISKI-CORS networks are available at <https://www.tusaga-aktif.gov.tr/>.

## REFERENCES

- Groves P.D; 2013: *Principles of GNSS. Inertial, and Multi-Sensor Integrated Navigation Systems (2nd ed.)*. Artech House, London, UK, 800 pp.
- Gučević J., Siniša D. and Olivera V.Š.; 2024: *Practical limitations of using the Tilt compensation function of the GNSS/IMU receiver*. Remote Sens., 16, 1327, doi: 10.3390/rs16081327.
- Hong S., Lee M.H., Chun H.H., Kwon S.H. and Speyer J.L.; 2005: *Observability of error states in GPS/INS integration*. IEEE Trans. Veh. Tech., 54, 731-743, doi: 10.1109/TVT.2004.841540.
- Jekeli C.; 2001: *Inertial Navigation Systems with geodetic applications*. De Gruyter, Berlin, Germany, 352 pp.
- Krzyżek R.; 2014: *Reliability analysis of the results of RTN GNSS surveys of building structures using indirect methods of measurement*. Geod. Cartogr., 63, 161-181, doi: 10.2478/geocart-2014-0012.
- Krzyżek R.; 2015a: *Algorithm for modelling coordinates of corners of buildings determined with RTN GNSS technology using vector translation method*. Art. Satell. J. Planet. Geod., 50, 115-125, doi: 10.1515/arsa-2015-0009.
- Krzyżek R.; 2015b: *Mathematical analysis of the algorithms used in modernized methods of building measurements with RTN GNSS technology*. Bol. Ciênc. Geod., 21, 848-866.
- Krzyżek R.; 2015c: *Modernization of the method of line-line intersection using RTN GNSS technology for determining the position of corners of buildings*. Art. Satell. J. Planet. Geod., 50, 41-57, doi: 10.1515/arsa-2015-0004.
- Krzyżek R.; 2017: *Evaluating the accuracy of determining coordinates of a corner of a building measured in the RTN GNSS mode, having applied the innovative algorithm of vector translation*. Rep. Geod. Geoinf., 103, 10-21, doi: 10.1515/rgg-2017-0002.
- Kurtovic Z. and Pagan R.; 2009: *A multi-mode active surveying pole*. European Patent Organisation, Munich, Germany.
- Luo X., Chen J. and Richter B.; 2017: *How Galileo benefits high-precision RTK - what to expect with the current constellation*. GPS World, 28, 22-28.

- Luo X., Schaufler S., Carrera M. and Celebi I.; 2018: *High-Precision RTK positioning with Calibration-Free Tilt Compensation*. In: Proc. FIG Congress 2018, Embracing our smart world where the continents connect: enhancing the geospatial maturity of societies, Istanbul, Turkey, 9407, 16 pp.
- Nichols M.E. and Talbot N.C.; 1996: *Pole-tilt sensor for surveyor range pole*. Trimble Navigation Limited, Sunnyvale, CA, USA, US Patent US5512905A, 7 pp.
- Pedley M.; 2012: *e-Compass: build and calibrate a tilt-compensating electronic compass*. Circuit Cellar, 265, 16-23.
- Pirtı A. and Yücel M.A.; 2023: *Evaluating the accuracy of determining coordinates of corners of the building surveyed in tilt technology*. KSCE J. Civ. Eng., 27, 2629-2636, doi: 10.1007/s12205-023-3309-5.
- Ponzo F.C., Auletta G., Ielpo P. and Ditommaso R.; 2024: *DInSAR–SBAS satellite monitoring of infrastructures: how temperature affects the “Ponte della Musica” case study*. J. Civil Struct. Health Monit., 14, 745-761, doi: 10.1007/s13349-023-00751-z.
- Positional Accuracy Handbook; 1999: *Using the National Standard for Spatial Data Accuracy (NSSDA) to measure and report geographic data quality*. Minnesota Planning and Land Management Information Center, St. Paul, MN, USA, 33 pp., <www.mnplan.state.mn.us/pdf/1999/lmic/nssda\_o.pdf>.
- Sveinung T.K., Jakob B.K. and Stewart G.R.; 2021: *Accuracy of Tilt-compensated GNSS sensors using Network-RTK*. Bachelor’s Thesis, Bachelor Geomatic’s Course, Department of Manufacturing and Civil Engineering, NTNU - Norwegian University of Science and Technology, Gjøvik, Norway, 60 pp., <ntnuopen.ntnu.no/ntnu-xmlui/bitstream/handle/11250/2782315/no.ntnu%3Ainspera%3A77257076%3A81956540.pdf?sequence=1>.
- Tersus GNSS; 2021: *Oscar GNSS receiver, extreme RTK with Tilt Compensation*. Tersus GNSS, Suite 58/11, Wilson St., South Yarra, VIC 3141, Australia, 102 pp., <www.tersus-gnss.com/product/oscar\_gnss\_receiver>.
- Titterton D. and Weston J.L.; 2004: *Strapdown inertial navigation technology (2nd ed.)*. American Institute of Aeronautics and Astronautics (AIAA), Education Series, Reston, VA, USA, 558 pp. doi: 10.1049/PBRA017E.
- Topcon; 2022: *HiPer VR*. Topcon Positioning Systems. Inc., Livermore, CA, USA, <www.topconpositioning.com/gnss-and-network-solutions/integrated-gnssreceivers/hiper-vr>.
- Wolf P.R. and Ghilani C.D.; 2008: *Elementary Surveying, an introduction to Geomatics*, 12th ed. Prentice Hall, Upper Saddle River, NJ, USA, 960 pp.
- Yang N. and Freestone J.; 2016: *High-performance GNSS antennas with phase-reversal quadrature feeding network and parasitic circular array*. In: Proc. 29th International Technical Meeting of the Satellites Division of the Institute of Navigation (ION GNSS+ 2016), Portland, OR, USA, pp. 364-372.
- Yang N. and Freestone J.; 2017: *Patch antenna with peripheral parasitic monopole circular arrays*. US Patent US20170047665A1. United States Patent and Trademark Office (USPTO), Alexandria, VA, USA.
- Yang N. and Gilbertson C.; 2016: *Wide and low-loss quadrature phase quad-feeding network for high-performance GNSS antenna*. US Patent US9343796B2. United States Patent and Trademark Office (USPTO), Alexandria, VA, USA.

Corresponding author: Atınc Pirtı  
Department of Geomatic Engineering, Yıldız Technical University  
Davutapasa street; 34220 Esenler, Istanbul, Turkey  
Phone: +90 212 3835300; e-mail: atinc@yildiz.edu.tr